

# Microstructural and Carbon Phase Analysis of Water Hyacinth Derived Biochar under Particle Size Variation

Dwi Amiliya Putri<sup>1</sup>, Yana Taryana<sup>2</sup> , Sigit Ristanto<sup>1</sup> , Nur Khoiri<sup>3</sup> , Affandi Faisal Kurniawan<sup>1\*</sup> 

<sup>1</sup>Faculty of Mathematics, Natural Sciences, and Information Technology Education, Universitas PGRI Semarang, Jl. Lontar No. 1 Semarang, Indonesia

<sup>2</sup>Research Centre for Telecommunication, National Research and Innovation Agency (BRIN), Bandung, Indonesia

<sup>3</sup>Graduate School of Universitas PGRI Semarang, Semarang, Indonesia

\* Corresponding author(s), e-mail: [affandifaisal@upgris.ac.id](mailto:affandifaisal@upgris.ac.id)

## Article Info:

### Article History:

received: 24 December 2025

accepted: 23 January 2026

available online: 26 January 2026

### Keyword:

biomass carbon, microstructure, particle size variation, SEM analysis, water hyacinth, XRD characterization

<https://doi.org/10.26877/lpt.v5i1.252>

Copyright © 2026 by author(s) and Lontar Physics Today. This work is licensed under the Creative Commons Attribution International License (CC BY 4.0).

<http://creativecommons.org/licenses/by/4.0/>



## Abstract:

Water hyacinth is an abundant lignocellulosic biomass with strong potential as a sustainable carbon source. This study aims to investigate the effect of particle size variation on the carbon phase and microstructural development of biomass-derived carbon from water hyacinth. The leaves of water hyacinth were used as raw material, thoroughly washed, cut into small pieces, and sun-dried for 11 days until completely dry. The dried leaves were then ground into powder and sieved into three particle-size fractions of 60, 80, and 100 mesh, with 75 g prepared for each sample. Carbonization was conducted using a furnace at 900°C for 1 h under a limited-oxygen environment. Carbon phase characterization was performed using X-ray diffraction (XRD), while surface microstructure analysis was carried out using Scanning Electron Microscopy (SEM). The results indicate that all samples exhibit a stable amorphous carbon phase, suggesting that particle size variation does not significantly influence carbon phase formation. However, particle size plays an important role in microstructural evolution, where finer particles promote more homogeneous morphology and enhanced pore development. These findings demonstrate that particle size acts as a microstructural control parameter without altering the resulting carbon phase, and they confirm the potential of water hyacinth leaves as a promising biomass precursor for carbon-based materials.

## 1. Introduction

Water hyacinth is a lignocellulosic biomass rich in cellulose, hemicellulose, and lignin, making it a highly promising raw material for conversion into carbon-based materials. Its biochemical composition typically consists of 20 - 35% cellulose, 15 - 30% hemicellulose, and 5 - 15% lignin on a dry-weight basis, all of which support its suitability for various thermochemical processes, including carbonization for producing biochar or activated carbon (Abba et al., 2025; Sanchez-Torres et al., n.d.). Carbon derived from biomass is widely utilized in advanced material applications such as electrodes, catalysts, and electromagnetic absorbers due to its lightweight, low cost, and renewable nature (Opia et al., 2021). One of the key factors influencing the quality of biomass-derived carbon is the particle size of the precursor prior to carbonization. Particle size affects the thermal homogeneity, devolatilization rate, and pore development, further determining the resulting microstructure and carbon phase (Peng et al., 2023; Zhang et al., 2024).

Characterization of microstructure and crystallinity is essential for understanding the quality and functional performance of carbon materials. Scanning Electron Microscopy (SEM) is used to examine

surface morphology, sheet thickness, and fragmentation level, while X-ray diffraction (XRD) provides information on the amorphous or semi-crystalline phases formed during pyrolysis. The combination of these two techniques enables a comprehensive evaluation of how particle size influences the evolution of internal structures in biomass-derived carbon (Permatasari et al., 2025; Wibawa et al., 2020).

Previous studies have shown that biomass-derived carbon typically exhibits an amorphous structure with small graphitic domains, although the extent of this characteristic strongly depends on carbonization conditions and the initial particle size of the biomass (Béguerie et al., 2022; Rigollet et al., 2025). Finer particles tend to produce more uniform heat distribution, which promotes pore formation and improves structural ordering. In contrast, larger particles often generate dense aggregates with incomplete fragmentation, resulting in heterogeneous surface morphology. However, studies specifically comparing the microstructure and carbon phase of water hyacinth biochar across different particle sizes remain limited (Hong et al., 2020).

This study focuses on analysing the effect of particle size variations 60 mesh, 80 mesh, and 100 mesh on the microstructural evolution and carbon phase of water hyacinth-derived carbon. Through SEM and XRD characterization, this research aims to clarify how particle size influences carbon morphology, fragmentation behavior, pore development, and structural uniformity while maintaining a stable amorphous carbon phase after carbonization. The findings are expected to demonstrate that particle size acts as a microstructural control parameter rather than a phase-determining factor, thereby providing scientific insight into the optimization of water hyacinth-based biocarbon for advanced material applications. This work contributes to the development of biomass-based carbon materials within the field of materials physics.

## 2. Theoretical Framework

### 2.2. *Carbon Structure*

Biomass such as water hyacinth serves as a natural carbon source rich in lignocellulosic components, particularly cellulose, hemicellulose, and lignin. These three components provide the fundamental framework for carbon formation during the pyrolysis process. When heated at high temperatures, the chemical bonds within the lignocellulosic matrix gradually break through devolatilization, releasing volatile compounds and leaving behind a solid carbon residue. At this stage, carbon atoms begin to associate and form an amorphous network lacking long-range structural order. This amorphous structure is characterized by the presence of small graphitic domains that are unevenly distributed and still contain residual oxygen functional groups within the carbon matrix (Jadhav & Dey, 2025). The particle size of the biomass plays a crucial role in determining the quality of the resulting carbon. Smaller particles possess a larger surface area and experience more uniform heat distribution, enabling the formation of a more homogeneous carbon structure. This condition also supports optimal pore development and sheet fragmentation during carbonization. Conversely, biomass with larger particle sizes often undergoes uneven heating, causing certain regions to remain partially uncarbonized, which leads to a more heterogeneous microstructure, the formation of larger aggregates, and non-uniform pore distribution (Zhou et al., 2020). These variations in particle size become a key factor in understanding the changes in physical properties and microstructural characteristics of biocarbon derived from water hyacinth.

## 2.2. Principle of X-Ray Diffraction (XRD)

XRD is a primary characterization technique used to analyse the crystal phases and degree of amorphousness in carbon materials. When X-rays are directed onto a sample, the interaction between the X-ray waves and the atomic arrangement produces a distinct diffraction pattern. Biomass-derived carbon typically exhibits a broad diffraction peak in the range of  $2\theta = 20^\circ - 30^\circ$ , which corresponds to the (002) graphitic plane. This broad peak indicates an irregular interlayer spacing and very small crystalline domains, classifying the resulting carbon structure as amorphous carbon (Murugesh, 2021).

## 2.3. Principle of Scanning Electron Microscopy (SEM)

SEM is used to examine the surface morphology, carbon sheet thickness, pore size, and the degree of particle fragmentation. In the context of biomass-derived carbon, SEM plays a crucial role in observing the transformation of the original cellulose-based structure into porous carbon sheets after the carbonization process. Carbon derived from smaller particle sizes (such as 100 mesh) typically exhibits thinner sheets, a more homogeneous structure, improved porosity, and more uniform fragmentation because heating and devolatilization occur more effectively throughout the material (Nurhilal et al., 2023). Conversely, samples with larger particle sizes (such as 60 mesh) tend to show large aggregates, denser surfaces, and lower porosity. This occurs due to uneven heat distribution, resulting in incomplete decomposition of certain regions. Consequently, the microstructure appears more massive and less developed, resembling graphene-like carbon that has not been well exfoliated (Fang et al., 2020). In this study, SEM analysis is used to compare the microstructural changes of carbonized water hyacinth across three different particle sizes, allowing a comprehensive evaluation of the relationship between particle size, pyrolysis behavior, and morphological development.

## 3. Method

### 3.1. Sample Preparation of Water Hyacinth

The preparation of water hyacinth samples consisted of several steps, including cutting, washing, drying, grinding, and sieving, as illustrated in Figure 1 (Zhou et al., 2020), which presents the flowchart of the carbonization and characterization process of water hyacinth biomass with particle size variation. The leaves used in this study were collected from the riverbank area in Sragi District, Pekalongan Regency. After collection, the leaves were thoroughly washed and dried under direct sunlight for 11 days until completely dehydrated. The dried leaves were subsequently ground using a household blender to obtain fine powder.

The resulting powder was sieved through 60, 80, and 100 mesh screens to produce uniform particle-size fractions. The variation in particle size was intentionally introduced as the independent variable to evaluate its influence on the structural and phase characteristics of the resulting biochar. For each particle-size fraction (60, 80, and 100 mesh), 75 g of dried water hyacinth powder was prepared as the initial mass to ensure consistency across all carbonization batches and to provide sufficient material for subsequent SEM and XRD characterization.

The dependent variables in this study comprise the structural and microstructural parameters obtained from XRD and SEM analyses. The XRD characterization was used to examine the diffraction pattern, including peak position ( $2\theta$ ), diffraction intensity (a.u.), and carbon phase characteristics, while

SEM analysis was conducted to observe the surface morphology and qualitative pore distribution of the biochar. Meanwhile, several parameters were maintained as controlled variables, including the initial sample mass, source of raw materials, carbonization conditions, and characterization procedures, to ensure the reliability and comparability of the results.

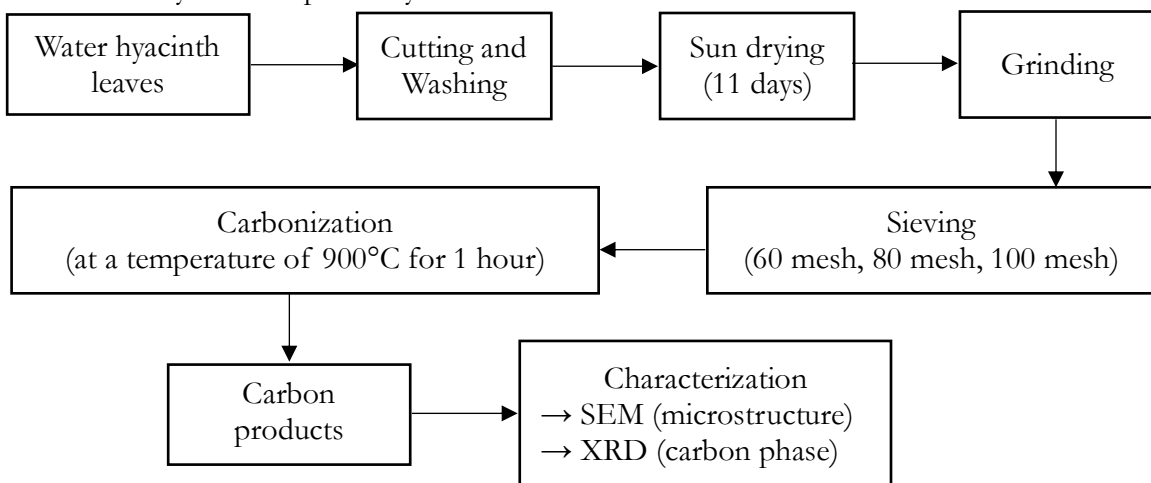


**Figure 1.** Flowchart of the carbonization and characterization process of water hyacinth biomass with particle size variation.

### 3.2. Carbonization Process

The water hyacinth powder was placed into a sealed cylindrical iron crucible designed specifically to limit oxygen exposure during carbonization. The crucible was equipped with a small pressure-relief pinhole on the lid, and the lid was secured tightly using a threaded locking cap. This configuration ensured that external air could not enter the crucible throughout the heating process, while the pinhole allowed volatile gases generated during devolatilization to escape in a controlled manner. Because the crucible was tightly sealed and had a limited internal volume, the small amount of oxygen initially present inside was rapidly consumed during the early phase of heating. Once this residual oxygen was depleted, the atmosphere within the crucible shifted into a stable low-oxygen (oxygen-limited) environment without requiring an inert gas flow. After the crucible was sealed, it was inserted into a horizontal furnace, and the temperature was increased from room temperature to 900°C at a controlled heating rate of 10°C/min. The furnace temperature was then maintained for 1 hour to complete the carbonization process. This heating profile supported consistent devolatilization and enabled uniform carbon development across all particle-size fractions. When carbonization was complete, the samples were left to cool naturally inside the furnace until they reached room temperature. The final mass of the carbon product obtained from each batch was approximately 8 grams, corresponding to a carbon yield of 10 - 11%, which is consistent with the typical mass loss behavior of lignocellulosic biomass undergoing high-temperature pyrolysis.

### 3.3. Characterization of Water Hyacinth Biochar

Microstructural characterization of carbonized water hyacinth was performed using a JEOL JSM-6510LA Scanning Electron Microscope (SEM) at the Integrated Laboratory of Diponegoro University. Observations were made at an accelerating voltage of 15 kV in Secondary Electron (SE) mode to obtain high-contrast images of the surface morphology. Several magnifications were used, including 50X, 200X, 500X, and 2000X, with the primary morphological interpretation based on the 2000X micrograph

presented in this study. Crystal structure characterization was performed using XRD at the National Research and Innovation Agency (BRIN) Bandung. Measurements were obtained with a Bruker D8 Advance diffractometer equipped with a  $Cu K\alpha$  radiation source ( $\lambda = 1.5406 \text{ \AA}$ ), operating at  $40 \text{ kV}$  and  $30 \text{ mA}$ . Diffraction data were collected over the range  $10^\circ - 80^\circ$  in  $2\theta$  with a step size of  $0.02^\circ$ , providing sufficient resolution to identify the amorphous and semi-crystalline characteristics typical of biomass-derived carbon. This study adopts the idealization that variations in particle size primarily influence heat transfer uniformity during carbonization but do not significantly alter the fundamental carbon phase formed. Therefore, similar XRD patterns across different mesh sizes are expected, with variations mainly observed in diffraction intensity rather than peak position. The accuracy of the XRD measurements is governed by the instrumental resolution and scanning parameters of the diffractometer. The Bruker D8 Advance system used in this study provides a typical angular resolution of approximately  $\pm 0.02^\circ$  in  $2\theta$ , corresponding to the selected step size. Minor variations in diffraction intensity may also arise from factors such as sample packing, surface flatness, and preferred orientation effects. As the objective of this study is focused on qualitative phase identification and comparative analysis among particle-size variations, these instrumental uncertainties do not significantly affect the interpretation of the carbon phase.

## 4. Result

### 4.1. X-Ray Diffraction Analysis

The XRD patterns of water hyacinth-derived carbon with particle sizes of 60, 80, and 100 mesh exhibit a dominant broad diffraction hump in the  $2\theta$  range of  $20^\circ - 30^\circ$ , indicating that all samples predominantly consist of amorphous carbon with small and poorly ordered graphitic domains, as shown in Figure 2. A prominent intensity maximum is observed at approximately  $2\theta = 30.18^\circ$  and appears consistently across all particle-size variations. This feature represents a broad amorphous scattering region rather than a sharp crystalline peak, reflecting the disordered nature of the carbon structure formed during pyrolysis.

At approximately  $2\theta = 30.18^\circ$ , the relative peak intensity for the 60, 80, and 100 mesh samples shows a clear increasing trend with decreasing particle size. The 100 mesh sample exhibits the highest relative intensity, followed by the 80 mesh and 60 mesh samples, indicating improved structural uniformity and scattering contribution in finer particles. Although the peak position remains unchanged for all samples, the variation in relative intensity suggests differences in structural coherence rather than changes in crystallographic phase. This trend confirms that particle size variation primarily affects scattering efficiency and microstructural coherence rather than inducing any crystallographic phase transformation.

The broad peak width indicates a reduced crystallite domain size and a high concentration of structural defects, which are characteristic of lignocellulosic biomass-derived carbon undergoing incomplete structural rearrangement during high-temperature carbonization (Hong et al., 2020; Murugesh, 2021). The diffraction intensity is expressed in arbitrary units (a.u.) because the analysis focuses on qualitative phase identification and comparative evaluation rather than absolute intensity quantification. Instrumental uncertainty and peak broadening effects are discussed in the Limitations section and are considered not to alter the qualitative phase interpretation presented here.

In addition to the dominant amorphous hump in the  $20^\circ - 30^\circ$  region, weak and diffuse intensity features are also observed at higher diffraction angles ( $> 30^\circ$ ). These features do not correspond to any distinct crystalline phases but instead represent background scattering from highly disordered carbon networks and residual inorganic constituents commonly present in biomass-derived carbon. Their broad and low-intensity nature indicates the absence of long-range structural ordering and therefore they are not interpreted as separate carbon phases. For this reason, the structural discussion is focused on the  $20^\circ - 30^\circ$  region, which is widely accepted as the primary indicator of amorphous or poorly ordered graphitic carbon in lignocellulosic materials.

These XRD characteristics do not indicate the formation of reduced graphene oxide. Confirmation of graphene-like structures would require additional techniques such as Raman spectroscopy or X-ray Photoelectron Spectroscopy (XPS) (Yuan et al., 2023). Therefore, the carbon phase in all samples is conservatively interpreted as amorphous carbon with minimal graphitic ordering.

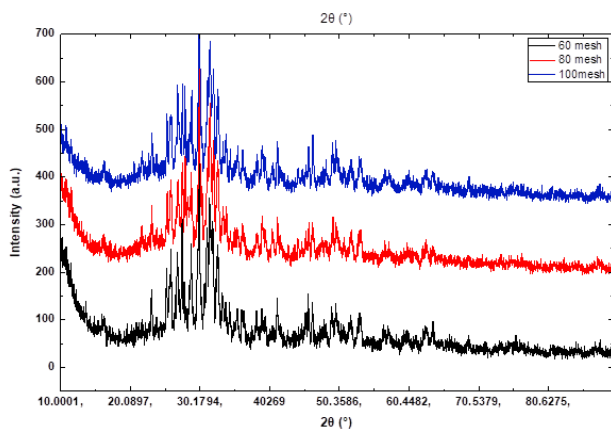


**Figure 2.** XRD patterns of water hyacinth-derived carbon with particle sizes of 60, 80, and 100 mesh, showing a dominant broad amorphous peak at approximately  $2\theta = 30.18^\circ$ . The relative diffraction intensity increases with decreasing particle size, where the 100 mesh sample exhibits the highest peak intensity, followed by 80 mesh and 60 mesh.

#### 4.2 Scanning Electron Microscope Analysis

##### Morphology of 60 Mesh Biomass-Derived Carbon

At the 60 mesh particle size, carbon is still dominated by large aggregates with thick, stacked sheets, as observed in the SEM micrograph at a magnification of  $2000 \times$ . Such morphology is commonly observed in coarse biomass-derived carbon that has not undergone optimal fragmentation during the grinding process. Larger biomass particles tend to possess dense structures with low porosity, resulting in reduced active surface area and less effective interaction with microwave waves (Ren et al., 2025). The coarse particle size also decreases available interfacial polarization pathways because the interlayer spacing is not formed optimally, thereby limiting the electromagnetic response of the material (Mu et al., 2024). This condition is consistent with the 60 mesh micrograph, which shows a rough surface with minimal pores, resembling densely packed and incompletely fragmented amorphous carbon. The dense structure restricts the development of interfacial polarization mechanisms.

### Morphology of 80 Mesh Biomass Derived Carbon

At the 80 mesh particle size, the particle structure begins to change more noticeably, as shown in Figure at a magnification of  $2000\times$ . The carbon sheets appear thinner and show reduced aggregation, allowing pores and gaps to emerge between the fragments (Goudarzi & Motlagh, 2019). This condition indicates that the grinding process is more effective compared to the 60 mesh sample, producing more reactive particles with a larger surface area. The increase in porosity and fragmentation helps enhance interfacial polarization and makes the material more responsive to microwave interaction. The more open structure also facilitates interactions between the carbon and the incoming waves, resulting in improved dielectric loss behavior at the 80 mesh particle size (Ma et al., 2023).

### Morphology of 100 Mesh Biomass Derived Carbon

At the 100 mesh particle size, the carbon appears much finer, more uniformly dispersed, and forms thin sheets with more distinct pore structures, as shown in Figure at a magnification of  $2000\times$ . This morphology indicates that the grinding process produced more homogeneous fragmentation, resulting in a significant increase in the material's accessible surface area. The thin, layered, and porous morphology reflects the formation of highly fragmented amorphous carbon, which is typical of finely ground biomass-derived carbon. Finely fragmented biomass carbon with a uniform pore distribution generally offers a larger active surface area, thereby supporting enhanced dipolar polarization processes and stronger electromagnetic wave interactions (Liu et al., 2023). This finding is consistent with (Chang et al., 2025), which notes that highly porous and ultra-fine carbon sheets can enhance dielectric loss mechanisms through abundant structural defects and interfacial polarization pathways.

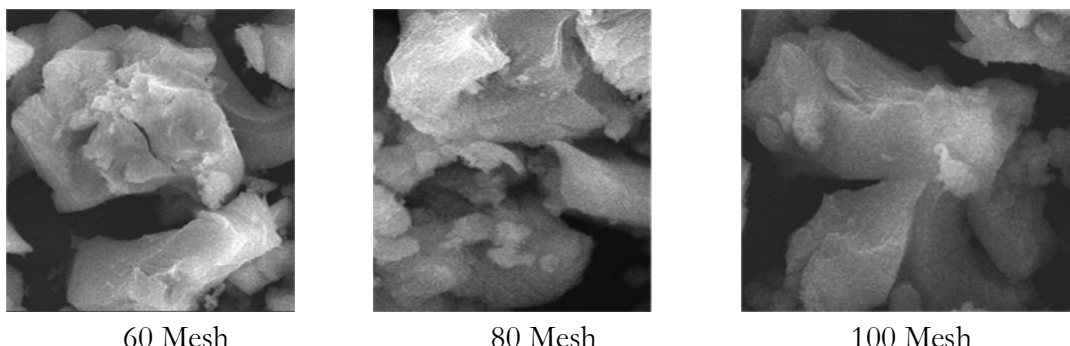


**Figure 3.** SEM micrographs of water hyacinth-derived carbon with particle sizes of (a) 60 mesh, (b) 80 mesh, and (c) 100 mesh at  $2000\times$  magnification, showing progressive fragmentation, sheet thinning, and pore development with decreasing particle size 3.

The more dispersed and pore-rich structure of the 100 mesh sample also allows multiple internal reflections (multiple scattering) when electromagnetic waves enter the material. This effect has been reported by (Zhou et al., 2020), who found that porous carbon with fine particle distribution increases the wave propagation path within the material, thereby improving energy attenuation. In the absence of direct microwave absorption measurements, the present study does not claim quantitative absorption performance. Instead, the observed microstructural features suggest that the 100 mesh carbon possesses structural characteristics that are favourable for porosity-driven multiple scattering and polarization-related mechanisms in microwave absorption systems. This interpretation is therefore based on

morphological inference rather than experimental validation of electromagnetic absorption properties.

#### *4.3 Integrated Interpretation of XRD and SEM Results*

The integrated interpretation of XRD and SEM results provides a comprehensive understanding of the relationship between carbon phase stability and microstructural evolution in water hyacinth-derived carbon. XRD analysis consistently reveals a broad diffraction peak centered around  $2\theta = 30^\circ$ , indicating that all samples retain a predominantly amorphous carbon structure regardless of particle size variation. The absence of sharp crystalline peaks confirms that particle size does not induce phase transformation during the carbonization process, suggesting that the fundamental carbonization pathway remains unchanged across all samples.

In contrast, SEM observations demonstrate a pronounced influence of particle size on the microstructural characteristics of the resulting carbon materials. Coarser particles exhibit relatively compact and irregular morphologies, while finer particles show progressive fragmentation, the formation of thinner carbon sheets, and increased pore development. This morphological evolution can be attributed to more uniform heat distribution and enhanced devolatilization in smaller particles during thermal decomposition, which promotes physical restructuring without altering the underlying carbon phase.

By correlating these findings, it becomes evident that particle size functions as a microstructural control parameter rather than a determinant of carbon phase formation. The stable amorphous phase identified by XRD reflects the thermochemical limitations inherent to lignocellulosic biomass precursors, while SEM reveals that physical morphology can be effectively tuned through particle size optimization. Similar integrated behaviors have been reported in previous studies, where biomass-derived carbon exhibited invariant amorphous phases alongside particle-size-dependent morphological refinement (Nurhilal et al., 2023; Zhou et al., 2020).

Overall, the combined XRD and SEM analyses indicate that phase stability and microstructural evolution operate through distinct but complementary mechanisms. While the carbon phase remains thermodynamically stable and insensitive to particle size variation, the microstructural features such as porosity, sheet formation, and surface roughness, are highly responsive to particle size. This integrated interpretation establishes a clear link between structural stability and morphological tunability, providing a solid experimental basis for the subsequent discussion on structure–property relationships.

## **5. Discussion**

### *5.1 Effect of Particle Size on the Carbon Phase (XRD Perspective)*

The XRD results indicate that carbon derived from water hyacinth exhibits a predominantly amorphous structure regardless of particle size variation. This finding suggests that the carbonization conditions applied in this study favour the formation of disordered carbon phases typical of lignocellulosic biomass, where complete graphitic ordering is limited. Similar amorphous characteristics have been widely reported in biomass-derived carbon systems subjected to high-temperature pyrolysis, where structural rearrangement remains incomplete due to the inherent complexity of the precursor material (Murugesh, 2021).

The absence of phase transformation across different particle sizes implies that particle size does not act as a determining factor for crystallographic phase evolution. Instead, the consistency of the

amorphous carbon phase reflects a stable thermochemical pathway during carbonization. This observation supports previous studies reporting that particle-size variation mainly affects physical and thermal processes rather than inducing fundamental changes in carbon bonding or lattice ordering (Gaurav et al., 2020). From a structural perspective, the XRD analysis confirms that the role of particle size is secondary to the carbonization temperature in determining the carbon phase. Consequently, the influence of particle size is more appropriately interpreted through its effect on microstructural development rather than crystallographic transformation, as further discussed in the integrated analysis section.

### *5.2 Effect of Particle Size on Carbon Morphology (SEM Perspective)*

SEM observations reveal that particle size plays a critical role in shaping the morphological features of water hyacinth-derived carbon. While all samples share the same amorphous carbon phase, clear differences in surface texture, fragmentation behavior, and pore development are evident across particle-size variations. These morphological differences reflect how initial particle size governs the physical restructuring of biomass during carbonization (Jadhav & Dey, 2025). Coarser particles tend to preserve denser carbon frameworks with limited fragmentation, which can be attributed to less uniform heat penetration during pyrolysis. In contrast, finer particles promote more homogeneous thermal exposure, leading to enhanced fragmentation and the formation of thinner carbon sheets accompanied by more evenly distributed pores. This behavior is consistent with previous reports indicating that smaller biomass particles facilitate more efficient devolatilization and structural reorganization during carbonization (Villardon et al., 2024).

These morphological trends suggest that particle size primarily influences the efficiency of microstructural refinement rather than altering the intrinsic carbon phase. The enhanced fragmentation and pore development observed in finer particles provide a microstructural basis for improved surface-related properties, reinforcing the interpretation that particle size functions as a morphological control parameter within a stable amorphous carbon framework (Yuan et al., 2023).

### *5.3 Relationship Between Microstructure and Carbon Phase on Material Properties*

From a materials perspective, the relationship between carbon phase and microstructural evolution in biomass-derived carbon is primarily governed by thermochemical stability rather than precursor particle size variation. The integrated interpretation of XRD and SEM results in this study indicates that all water hyacinth-derived carbon samples share a stable amorphous carbon framework, while particle size variation primarily governs microstructural evolution rather than phase transformation. This observation supports previous studies reporting that biomass-derived carbon generally remains amorphous after carbonization, with structural ordering being limited by the intrinsic nature of lignocellulosic precursors and carbonization conditions rather than precursor size alone.

The consistency of the carbon phase identified by XRD across all samples indicates that particle size does not significantly influence the fundamental carbonization pathway. Instead, SEM observations reveal that particle size affects the physical restructuring of carbon during thermal decomposition, including fragmentation behavior, sheet formation, and pore development. Similar trends have been reported in earlier works, where finer biomass particles facilitated more homogeneous heat distribution and enhanced devolatilization, resulting in more porous and uniformly structured carbon materials (Nurhilal et al., 2023). This integrated behavior suggests that particle size functions as a microstructural

control parameter rather than a phase-determining factor. Such a relationship has also been highlighted by Zhou et al. and Nurhilal et al., who emphasized that porous morphology and thin carbon sheet formation play a critical role in enhancing surface-related properties of biomass-derived carbon without altering its amorphous nature (Zhou et al., 2020). Therefore, the integration of XRD and SEM analyses confirms that the carbon system remains within a stable amorphous regime, while particle size variation provides an effective strategy for tailoring microstructural characteristics. This finding aligns with previous literature and reinforces the role of particle size optimization in improving the functional potential of biomass-derived carbon materials.

#### *5.4 Limitations of the Study*

This study provides a fundamental insight into the relationship between biomass particle size and the resulting carbon phase and microstructural characteristics of water hyacinth-derived carbon. Nevertheless, several limitations should be acknowledged to ensure a balanced interpretation of the findings and to define the scope of the conclusions drawn.

First, the characterization approach adopted in this work is predominantly qualitative, focusing on phase identification and morphological comparison. Quantitative measurements of specific surface area and pore characteristics, such as Brunauer Emmett Teller (BET) analysis, were not conducted. Consequently, the influence of particle size on porosity-related parameters could not be quantitatively correlated with the observed microstructural features. Second, Raman spectroscopy was not employed, which limits a more detailed evaluation of structural disorder through parameters such as the ID/IG ratio and constrains direct comparison with graphitic or graphene-like carbon references.

Furthermore, SEM observations were limited to qualitative morphological interpretation without image-based statistical analysis, such as pore-size distribution or quantitative evaluation of carbon sheet thickness. Despite these limitations, the primary objective of this study to elucidate the role of particle size in governing carbon phase stability and microstructural evolution remains valid. Rather than diminishing the significance of the results, these limitations highlight opportunities for future work aimed at establishing stronger structure–property relationships in biomass-derived carbon materials.

#### *5.5 Research Implications and Development Suggestions*

This study emphasizes the strength of a simple, systematic, and reproducible approach for evaluating biomass-derived carbon through clearly defined variables and accessible characterization techniques. By establishing particle size as the primary independent variable and correlating it with carbon phase stability and microstructural evolution using combined XRD and SEM analyses, this work provides a robust framework for assessing carbon quality without relying on complex or highly specialized instrumentation.

From a materials physics perspective, the integration of XRD and SEM allows the separation between crystallographic stability and microstructural development to be clearly identified. While the amorphous carbon phase remains stable under identical carbonization conditions, particle size acts as an effective microstructural control parameter that governs fragmentation behavior, sheet formation, and pore development. This distinction is important for interpreting structure–property relationships in biomass-derived carbon systems and can serve as a reference model for similar thermochemical studies.

Beyond water hyacinth, the methodological framework presented in this study can be readily extended to other non-edible or underutilized biomass sources, including invasive plants and agricultural residues. Such an approach supports broader applications in sustainable materials research by enabling

preliminary screening of carbon phase stability and microstructural quality using widely available laboratory facilities. In the context of Indonesia and other biomass-rich regions, this strategy offers a pathway to utilize abundant non-food biomass resources for functional carbon materials without competing with food security needs.

Future studies may build upon this framework by incorporating quantitative surface area analysis, spectroscopic evaluation of structural disorder, and functional performance testing to further refine the relationship between microstructure and material properties. Nevertheless, the present study establishes a solid methodological foundation for reproducible and scalable biomass carbon characterization.

## 6. Conclusion

This study demonstrates that variations in the particle size of water hyacinth leaves do not alter the fundamental carbon phase produced through carbonization, which consistently remains amorphous under identical processing conditions. This conclusion is supported by the absence of sharp diffraction peaks at approximately  $26^\circ$  (002) and  $43^\circ$  (100) in the XRD patterns, which are characteristic of crystalline or graphene-like carbon, as well as the lack of layered stacking or ordered sheet features in the SEM images. Instead, particle size plays a decisive role in governing microstructural evolution, influencing fragmentation behavior, sheet formation, and pore development as revealed through integrated SEM and XRD analyses.

The combined interpretation of structural and morphological characterization confirms that particle size functions as a microstructural control parameter rather than a phase-determining factor. Finer particle sizes promote more homogeneous thermal decomposition and more refined porous structures, while coarser particles tend to retain denser and less fragmented morphologies. This distinction is critical for understanding structure–property relationships in biomass-derived carbon materials.

Beyond the specific case of water hyacinth, this work highlights the strength of a reproducible and accessible characterization framework for evaluating carbon materials derived from non-edible biomass. The approach presented in this study can be readily applied to other biomass sources, supporting sustainable material development without competing with food resources. Overall, the findings contribute to the broader field of materials physics by providing a clear methodological basis for correlating particle size, microstructure, and carbon phase stability in biomass-derived carbon systems.

## Authors Contribution

**Dwi Amiliya Putri:** Conceptualization, Methodology, Investigation, Formal analysis, Visualization, Writing – original draft, Writing – review & editing. **Yana Taryana:** Investigation, Validation, Writing – review & editing. **Sigit Ristanto:** Resources, Conceptualization, Supervision, Writing – review & editing. **Nur Khoiri:** Supervision, Validation, Writing – review & editing. **Affandi Faisal Kurniawan:** Conceptualization, Supervision, Validation, Writing – review & editing. All authors have reviewed and approved the final manuscript and agreed to the order of authorship.

## Funding Statement

This research was funded by the Institute of Research and Community Service (LPPM), Universitas PGRI Semarang, Indonesia.

## Acknowledgements

The authors gratefully acknowledge the financial support provided by LPPM Universitas PGRI Semarang. Appreciation is also extended to the Research Centre for Electronics and Telecommunication, BRIN Bandung, for granting access to the XRD characterization facilities.

## Ethical statement

This study did not involve human participants, personal data, or animal subjects. All experimental procedures were limited to the preparation and characterization of biomass-derived carbon materials using water hyacinth (*Eichhornia crassipes*). Therefore, approval from an institutional ethics committee was not required. The collection and use of water hyacinth complied with local environmental guidelines and posed no ethical, ecological, or biosafety concerns. No sensitive, hazardous, or regulated biological materials were used in this research.

## Declaration of AI use

The authors used AI tools (ChatGPT, OpenAI) to translate text from Indonesian to English, to improve paragraph clarity and organization, to check for potential typographical errors, and to paraphrase sentences for better readability without altering the scientific substance. All AI-assisted outputs were thoroughly reviewed, adjusted, and validated by the authors. The authors remain fully responsible for the accuracy, originality, and scientific integrity of this manuscript. No data, images, or analyses were generated by AI.

## Conflict of Interest

**Sigit Ristanto** and **Affandi Faisal Kurniawan** serve as Section Editors of the journal. To avoid any potential conflict of interest, the editorial handling of this manuscript, including reviewer selection, peer-review management, and editorial decision-making, was conducted by an independent editor in accordance with the journal's standard procedures. The authors declare no other competing interests.

## Supplementary Materials and Data Availability

The SEM images, XRD raw data, and supporting characterization notes used in this study are available from the corresponding author upon reasonable request. All shared data will be anonymized and provided in accordance with institutional regulations. No external repository is used for this dataset.

## References

Abba, A., Sabarinath, S., & Mustapha, R. A. (2025). Advancing circular bioeconomy through systematic review of multi-product biorefinery approaches for water hyacinth based renewable energy. *iScience*. <https://doi.org/10.1016/j.isci.2025.112807>

Béguerie, T., Weiss-Hortala, E., & Nzihou, A. (2022). Calcium as an innovative and effective catalyst for the synthesis of graphene-like materials from cellulose. *Scientific Reports*, 12(1), 21492. <https://doi.org/10.1038/s41598-022-25943-3>

Chang, Q., Xie, Z., Chen, G., Li, Z., Duan, Y., Shi, B., & Wu, H. (2025). Enhancement in conduction loss induced by morphology engineering for excellent electromagnetic wave absorption. *Journal of Materomics*, 11(4), 100927. <https://doi.org/10.1016/j.jmat.2024.100927>

Fang, Y., Xue, W., Zhao, R., Bao, S., Wang, W., Sun, L., Chen, L., Sun, G., & Chen, B. (2020). Effect of nanoporosity on the electromagnetic wave absorption performance in a biomass-templated

Fe<sub>3</sub>O<sub>4</sub>/C composite: A small-angle neutron scattering study. *Journal of Materials Chemistry C*, 8(1), 319–327. <https://doi.org/10.1039/C9TC04569D>

Gaurav, G. K., Mehmood, T., Cheng, L., Klemeš, J. J., & Shrivastava, D. K. (2020). Water hyacinth as a biomass: A review. *Journal of Cleaner Production*, 277, 122214. <https://doi.org/10.1016/j.jclepro.2020.122214>

Goudarzi, R., & Motlagh, G. H. (2019). The effect of graphite intercalated compound particle size and exfoliation temperature on porosity and macromolecular diffusion in expanded graphite. *Heliyon*, 5(10). <https://doi.org/10.1016/j.heliyon.2019.e02595>

Hong, Z., Zhong, F., Niu, W., Zhang, K., Su, J., Liu, J., Li, L., & Wu, F. (2020). Effects of temperature and particle size on the compositions, energy conversions and structural characteristics of pyrolysis products from different crop residues. *Energy*, 190, 116413. <https://doi.org/10.1016/j.energy.2019.116413>

Jadhav, R. H., & Dey, A. (2025). Pre-Treatment and Characterization of Water Hyacinth Biomass (WHB) for Enhanced Xylose Production Using Dilute Alkali Treatment Method. *Water*, 17(3), 301. <https://doi.org/10.3390/w17030301>

Liu, Z., Su, S., Zhao, Y., Wang, L., & Wang, Y. (2023). Multi-morphology composite: Particle & petal-shaped ZnFe<sub>2</sub>O<sub>4</sub>/flower-shaped ZnO@ Porous biomass carbon with excellent broadband microwave absorption performance. *Carbon*, 215, 118448. <https://doi.org/10.1016/j.carbon.2023.118448>

Ma, L., Wu, Y., Wu, Z., Xia, P., He, Y., Zhang, L., Fan, H., Tong, C., Zhang, L., & Gao, X. (2023). Enhanced dielectric loss in N-doped three-dimensional porous carbon for microwave absorption. *Materials Today Advances*, 20, 100434. <https://doi.org/10.1016/j.mtadv.2023.100434>

Mu, Z., Xie, P., A. Alshammari, D., Kallel, M., Liang, G., Yu, Z., El-Bahy, Z. M., & Mao, Z. (2024). From structure to function: Innovative applications of biomass carbon materials in microwave absorption. *Advanced Composites and Hybrid Materials*, 7(6), 220. <https://doi.org/10.1007/s42114-024-01020-3>

Murugesh, V. (2021). Chemical Analysis of Water Hyacinth Ash by XRD and SEM. *Indian Journal of Advanced Botany (IJAB)*, 1(1), 8–10. <https://doi.org/10.35940/ijb.B2003.041121>

Nurhilal, O., Hidayat, S., Sumiarsa, D., & Risdiana, R. (2023). Natural biomass-derived porous carbon from water hyacinth used as composite cathode for lithium sulfur batteries. *Sustainability*, 15(2), 1039. <https://doi.org/10.3390/su15021039>

Opia, A. C., Kameil, A. H. M., Syahrullail, S., Abd Rahim, A. B., & Johnson, C. A. N. (2021). Eichhornia crassipes transformation from problems to wide unique source of sustainable materials in engineering application. *IOP Conference Series: Materials Science and Engineering*, 1051(1), 12100. <https://doi.org/10.1088/1757-899X/1051/1/012100>

Peng, J., Kang, X., Zhao, S., Yin, Y., Zhao, P., Ragauskas, A. J., Si, C., & Song, X. (2023). Regulating the properties of activated carbon for supercapacitors: Impact of particle size and degree of aromatization of hydrochar. *Advanced Composites and Hybrid Materials*, 6(3), 107. <https://doi.org/10.1007/s42114-023-00682-9>

Permatasari, G. T., Mas'udah, K. W., Asih, R., Astuti, F., Nurdiansah, H., Noerochim, L., & Darminto, D. (2025). Structural Analysis of Palm Kernel Shell-Derived Biomass as a Carbon-Based Anode Material for Dual Carbon Battery. *IOP Conference Series: Earth and Environmental Science*, 1488(1), 12014. <https://doi.org/10.1088/1755-1315/1488/1/012014>

Ren, X., Zhen, M., Meng, F., Meng, X., & Zhu, M. (2025). Progress, Challenges and Prospects of Biomass-Derived Lightweight Carbon-Based Microwave-Absorbing Materials. *Nanomaterials*, 15(7), 553. <https://doi.org/10.3390/nano15070553>

Rigollet, S., Béguerie, T., Weiss-Hortala, E., Flamant, G., & Nzihou, A. (2025). Synthesis of graphitic biocarbons from lignin fostered by concentrated solar energy. *Scientific Reports*, 15(1), 6418. <https://doi.org/10.1038/s41598-025-91204-8>

Sanchez-Torres, R., Bustamante, E. O., López, T. P., & Espindola-Flores, A. C. (2025). Efficiency Determination of Water Lily (*Eichhornia crassipes*) Fiber Delignification by Electrohydrolysis Using Different Electrolytes. *Recycling*. <https://doi.org/10.3390/recycling10040130>

Villardon, A., Alcazar-Ruiz, A., Dorado, F., & Sanchez-Silva, L. (2024). Enhancing carbon dioxide uptake in biochar derived from husk biomasses: Optimizing biomass particle size and steam activation conditions. *Journal of Environmental Chemical Engineering*, 12(5), 113352. <https://doi.org/10.1016/j.jece.2024.113352>

Wibawa, P. J., Nur, M., Asy'ari, M., & Nur, H. (2020). SEM, XRD and FTIR analyses of both ultrasonic and heat generated activated carbon black microstructures. *Helijon*, 6(3). <https://doi.org/10.1016/j.heliyon.2020.e03546>

Yuan, S.-J., Wang, J.-J., Dong, B., & Dai, X.-H. (2023). Biomass-derived carbonaceous materials with graphene/graphene-like structures: Definition, classification, and environmental applications. *Environmental Science & Technology*, 57(45), 17169–17177. <https://doi.org/10.1021/acs.est.3c04203>

Zhang, J., Wang, Z., Dai, G., Heberlein, S., Chan, W. P., Wang, X., Tan, H., & Lisak, G. (2024). Assessing the effect of size and shape factors on the devolatilization of biomass particles by coupling a rapid-solving thermal-thick model. *Journal of Analytical and Applied Pyrolysis*, 183, 106835. <https://doi.org/10.1016/j.jaap.2024.106835>

Zhou, X., Jia, Z., Feng, A., Wang, K., Liu, X., Chen, L., Cao, H., & Wu, G. (2020). Dependency of tunable electromagnetic wave absorption performance on morphology-controlled 3D porous carbon fabricated by biomass. *Composites Communications*, 21, 100404. <https://doi.org/10.1016/j.coco.2020.100404>